Nonrelativistic *ab initio* calculation of the interaction potentials between metastable Ne atoms

S. Kotochigova
National Institute of Standards and Technology, Gaithersburg, Maryland 20899

E. Tiesinga
Department of Chemistry and Biochemistry, University of Maryland, College Park, Maryland 20742

I. Tupitsyn
Physics Department, St. Petersburg University, St. Petersburg 198904, Russia

(Received 24 May 1999; published 17 March 2000)

We compute nonrelativistic *ab initio* electronic potential surfaces for two metastable $2p^5\,3s$ neon atoms using a multiconfiguration all-electron valence-bond method. Spectroscopic constants and long-range C_6 dispersion coefficients are presented for ${}^{3,5}\Sigma_{g/u}$, ${}^{3,5}\Pi_{g/u}$, and ${}^{1,3,5}\Delta_{g/u}$ symmetries. In addition, we analyze the role of various atomic configurations in the formation of the neon dimer. Our results can be used to model the suppression of collision-induced ionization of metastable neon, which is believed to be a good candidate for Bose-Einstein condensation.

PACS number(s): 34.20.Mq, 31.15.Ar, 32.80.Pj

I. INTRODUCTION

Laser-cooled metastable noble-gas atoms have recently gained attention as systems in which associative or Penning ionization [1], ultracold collision physics [2], high-precision photoassociation spectroscopy [3], and possibly Bose-Einstein condensation with polarized metastable atoms [4,2] can be studied. In order to successfully describe these processes, which rely on modeling of the relative nuclear motion, the electronic potential energy surfaces between two metastable noble-gas atoms need to be evaluated. These curves will determine bond lengths, dissociation energies, and dispersion coefficients, as well as curve crossings and anticrossings.

In this paper a multiconfiguration valence-bond method is used to calculate non-relativistic *ab initio* electronic potentials of two metastable neon $1s^2\,2s^2\,2p^5\,3s(^3P)$ atoms. For brevity we often omit the term $1s^2\,2s^2$ and only use the abbreviation $2p^5\,3s$ in order to describe a metastable neon atom. Metastable neon is the lightest noble-gas atom with an electronic structure where many-electron correlation and polarization effects play an important role in atom-atom interactions and hence forms a challenge for any electronic structure calculation. The advantage of the valence-bond method is that it is inherently well suited for collisional problems. It is able to describe the separated atom limit exactly. In addition we find that the all-electron core and nonorthogonal multiconfiguration interaction procedure converges sufficiently well for short- and intermediate-range internuclear separations.

Our potential energy surfaces give insight into the possibility of being able to hold polarized metastable neon in magnetic or optical traps. This situation can only be realized if associative or Penning ionization of interacting polarized atoms is suppressed. Such suppression, predicted for the quintet ${}^5\Sigma_g$ potential of the metastable helium dimer [4], cannot be guaranteed for Ne because of its more complicated electronic structure. Nevertheless, the ${}^5\Lambda$ ($\Lambda=\Sigma,\Pi,\ldots$) molecular states formed from two metastable Ne atoms are the best candidates for suppression as these symmetries cannot autoionize. Similar to metastable helium, this suppression of the ionization follows from the observation that the only energetically accessible $Ne^+ + Ne$ potentials involve a $2p^5$ ion and a $2p^6$ neutral atom. Now the total electron spin of this ionic dimer plus a free electron can only be zero or 1. Hence, the ionization process of a ${}^5\Lambda$ state, which must conserve the total electron spin, is prohibited.

Loss of metastable atoms from a magnetic or optical trap can nevertheless occur via other collisional processes. The multiplet structure of the ${}^5\Lambda$ potentials may cause depolarization [2] and relativistic spin-orbit interactions coupling the ${}^5\Lambda$ symmetries to autoionizing ${}^3\Lambda$ and ${}^1\Lambda$ states cause additional loss of polarized atoms. This loss is controlled by the complete shape of the interatomic potentials and hence the short-range interactions are needed.

Earlier theoretical pseudopotential studies of Ne_2 describe the interaction between a ground-state $2p^6$ and a metastable atom [5,6]. Recently, the long-range form of the potentials between two metastable Ne atoms has been predicted semiempirically from known atomic properties [2]. The short-range molecular structure of Ne_2 in the metastable $2p^5 3s + 2p^5 3s$ or any other excited state, however, is not available from either experiment or theory.

We describe an explicit multiconfiguration all-electron calculation of ${}^5\Lambda_{g/u}$, ${}^3\Lambda_{g/u}$ ($\Lambda=\Sigma$, Π, and Δ), and ${}^1\Delta_g$ potential curves dissociating to the metastable atomic limits of Ne_2 for R between $3a_0$ and $50a_0$ ($1a_0=0.052\,917\,7$ nm). The (energetically lowest) quintet symmetries, ${}^5\Sigma_{g/u}$, ${}^5\Pi_{g/u}$, and ${}^5\Delta_{g/u}$, are of particular interest. In our calculation we focus on obtaining the multiplet structure of the quintet potentials but we also present the triplet and some of the singlet potentials to elucidate their structure.

A discussion of the relativistic interactions falls outside the scope of the paper. To take into account the fine-structure effects such as spin-orbit interaction one has to either develop and apply a relativistic method from first principles or

use perturbation theory. The first way is much more challenging than the second. As far as we know, there exists no *ab initio* relativistic treatment of the excited Ne_2 molecule. This *ab initio* treatment is one of our future goals. To apply perturbation theory for fine-structure splittings one can use our non-relativistic potentials as a starting point. In a Ne atom the splitting between $3s$ and $3s'$ with the same total angular momentum $J=1$ is still three times bigger than the fine-structure splittings and spin-orbit effects, even though important for a collision, can be introduced perturbatively.

In a nonrelativistic framework the electronic potential curves are labeled by $^{2S+1}\Lambda_{g/u}$. The quantity S is the total electron spin and Λ is the projection along the internuclear axis of the total electron mechanical angular momentum L. The gerade or ungerade label reflects the symmetry of the electron wave function under inversion around the center of charge.

The remainder of the paper is organized as follows: In Sec. II we briefly review our version of the multiconfiguration valence-bond method. Sec. III discusses the molecular basis used in the calculation. In the two subsequent sections we present and discuss the results of the calculations. We give both potentials, spectroscopic constants, dispersion coefficients, and an analysis of the configuration weights as a function of internuclear separation in order to follow the formation of the molecule. The quintet symmetries are discussed in Sec. IV and all triplets and $^1\Delta$ symmetries in Sec. V. We end with some conclusions in Sec. VI.

II. METHOD

The valence-bond (VB) theory was initially developed by Heitler and London [7] to calculate the electronic structure of the H_2 molecule. The essence of this method is to express the molecular wave function as a linear combination of localized atomic wave functions. The generalization of this method for heavier molecules is reviewed in the book by McWeeny [8], where it has been proven to be efficient for intermediate and large or asymptotic internuclear separation. In the VB approach each pair of interacting electrons of a molecule is described with a product of two orbitals centered at either nuclei. The molecular wave function is then constructed from Slater determinants of these electronic orbitals, which ensures that the Pauli principle is automatically satisfied. The VB approach is appropriate for asymptotic R, since for increasing R the molecular VB wave functions become more and more localized, eventually transforming into atomic orbitals. Alternative approaches such as the molecular orbital (MO) and Hartree-Fock (HF) methods [9–11] use descriptions of molecular orbitals containing two electrons. This introduces doubly occupied orbitals for all internuclear separations R, whereas in the asymptotic region the quasimolecule should dissociate to two singly occupied orbitals that do not overlap. Thus the HF and MO methods are poor approximations to the true molecular wave function for large internuclear separations.

The next stage in the development of the VB method was to introduce self-consistency at each R in a manner similar to the HF method, but now with more realistic VB wave functions. This approach was named the generalized valence bond (GVB) method and developed successfully in a series of studies [12–15]. In these early GVB implementations, however, the orbitals are based on Gaussian functions.

We present results of our version of the VB method [16–18], where we have modified and developed the earlier approaches by using a nonorthogonal basis set of Hartree-Fock and Sturmian functions [19,20] instead of simple analytical functions [12–15]. The Hartree-Fock atomic determinant wave functions describe the occupied orbitals and both Hartree-Fock and Sturmian functions the unoccupied (virtual) orbitals. This ensures that the configuration interaction (CI) expansion converges quickly. In general, the VB solution can be unstable for short R, because the basis functions become linearly dependent so that small errors in matrix elements of the Coulomb and exchange interactions and in the nonorthogonality or overlap matrix can produce large errors in the total energy of a molecule. Therefore the conventional opinion is that the HF method for small internuclear separations provides better results than the VB method. In our model we avoid this kind of instability by calculating the matrix elements with high accuracy and using a CI with a nonorthogonal basis set. Another important feature of our approach is that we perform an all-electron calculation instead of the widely used pseudopotential methods.

The total molecular wave function Ψ_{AB} in our approach is given by a linear combination of Slater determinants $\det_\alpha$ corresponding to various configurations of the molecule

$$\Psi_{AB}(\vec{r}) = \sum_\alpha C_\alpha \det_\alpha(\vec{r}), \tag{1}$$

where $\vec{r}$ describes the electron coordinates. In turn, each molecular configuration is constructed from one configuration of atom A and one of atom B. The molecular configurations form a nonorthogonal basis and therefore the electronic wave functions of the molecule must be found from solving a generalized eigenvalue problem

$$\hat{H}_{AB}\vec{C} = E\hat{S}_{AB}\vec{C}, \tag{2}$$

where $\hat{S}_{AB}$ is the nonorthogonality overlap matrix and $\hat{H}_{AB}$ is the electronic Hamiltonian matrix, which includes both Coulomb and exchange electron-electron interactions as well as electron-nuclei interactions.

For each bonding pair of electrons, where the two electron orbitals are localized on different centers, two-center Coulomb, exchange integrals, and overlap matrix elements are calculated using a symmetric reexpanding procedure developed in Ref. [16]. The localized electron orbitals are either Hartree-Fock atomic or Sturmian orbitals. These latter orbitals are crucial in describing the molecular correlation. The orbitals replace highly excited Hartree-Fock atomic orbitals that are too diffuse to be used in a CI. The Sturmian functions are found by solving the Sturmian equation with an energy corresponding to the energy of occupied valence orbitals. The solutions, which include both continuum and discrete parts of the electron spectra form a complete set.

III. OVERVIEW OF MOLECULAR BASIS

For each atom self-consistent Hartree-Fock atomic orbitals belonging to the $1s^2$, $2s^2$, $2p^5$, and $3s$ configurations are used to create a multiconfiguration basis set for the metastable Ne_2 molecule. In addition, Hartree-Fock virtual or unoccupied orbitals designated by $3p$, $3d$, $4s$, $4p$, $4d$, $5p$, and $5d$ are included. Using Sturmian functions for these virtual orbitals proved to be less accurate.

For ultracold collisions the modification of the closed shells $1s^2\,2s^2$ due to the presence of the second atom is negligible and we are justified in describing the effect of these orbitals in terms of a frozen core potential that is felt by the remaining valence electrons. The core potential is calculated exactly from Coulomb and exchange interactions between all electrons of core *A* and *B*. The $2p^5$, one-electron excitations out of the $2p^5$ shell and $3s$, $3p$, $3d$, $4s$, $4p$, $4d$, $5p$, and $5d$ orbitals form the valence orbitals. Various covalent and ionic configurations are constructed from these atomic valence orbitals. In total we have included 89 such configurations in our basis set. This particular choice of configurations was obtained after testing different basis sets and takes into account the majority of the correlation but simultaneously keeps the number of one- and two-electron integrals manageable.

The complete list of configurations is given in Table I. The configurations have been divided into several classes based on their role in the molecular formation. The first line in the table describes the core electrons. All other lines in Table I describe the valence configurations. The first class of valence configurations contains the configuration of two metastable Ne atoms. This metastable configuration is expected to play the leading role in the configuration interaction expansion of the metastable potentials.

The next class describes configurations where one of the atoms is in the metastable state and the other is in a higher excited state with the same parity as the first atom. These configurations improve the description of the metastable atom and hence the molecule at large internuclear separation. The configurations ensure that the molecule dissociates correctly. The class labeled with ''opposite parity'' describes molecular configurations with a parity that is opposite to the configurations of the previous class. Again one of the atoms is in the metastable state. These configurations only contribute to the formation of the metastable molecule at short and intermediate internuclear separation.

The next two valence classes give rise to the long-range polarization interactions between neutral metastable atoms. The ''C_6'' configurations lead to the induced dipole-dipole $-C_6/R^6$ interaction and the ''C_8'' configurations lead to the induced dipole-quadrapole interaction. Additional covalent configurations are constructed from one ground-state $2p^6$ atom and an excited atom. The last two classes describe ionic $Ne^+ + Ne^-$ configurations where the Ne^+ ion is in its ground-state configuration. The term ''ionic'' is somewhat misleading. These states are not truly ionic in that the additional electron of the Ne^- atom is still bound to the neutral $2p^6$ atom. However, these configurations do allow us to de-

TABLE I. The molecular configurations used in the calculations. Notice that not all configurations are listed. When the atomic configurations for a specific molecular configuration are different, the inverted configuration is not listed. However, they are included in the actual calculation. The description of the configurations is explained in the text.

Atom A + Atom B	Description
$1s^2\,2s^2 + 1s^2\,2s^2$	Core
$2p^5\,3s + 2p^5\,3s$	Metastable
$2p^5\,4s + 2p^5\,3s$	Atomic (same parity)
$2p^5\,3d + 2p^5\,3s$	
$2p^5\,4d + 2p^5\,3s$	
$2p^5\,5d + 2p^5\,3s$	
$2p^4\,3s3p + 2p^5\,3s$	
$2p^4\,3s4p + 2p^5\,3s$	
$2p^5\,3p + 2p^5\,3s$	Atomic (opposite parity)
$2p^5\,4p + 2p^5\,3s$	
$2p^5\,5p + 2p^5\,3s$	
$2p^4\,3s^2 + 2p^5\,3s$	
$2p^4\,3s3d + 2p^5\,3s$	
$2p^4\,3d4s + 2p^5\,3s$	
$2p^5\,3p + 2p^5\,3p$	C_6
$2p^5\,3p + 2p^5\,4p$	
$2p^5\,3p + 2p^5\,5p$	
$2p^5\,4p + 2p^5\,4p$	
$2p^5\,4p + 2p^5\,5p$	
$2p^5\,3p + 2p^5\,3d$	C_8
$2p^5\,3p + 2p^5\,4d$	
$2p^5\,4p + 2p^5\,4d$	
$2p^5\,3s + 2p^6$	Other neutral
$2p^5\,3p + 2p^6$	
$2p^5\,3d + 2p^6$	
$2p^5\,4s + 2p^6$	
$2p^5\,4p + 2p^6$	
$2p^5 + 2p^5\,3s^2$	Ionic
$2p^5 + 2p^5\,3p^2$	
$2p^5 + 2p^5\,3d^2$	
$2p^5 + 2p^5\,3s3p$	
$2p^5 + 2p^5\,3p3d$	
$2p^5 + 2p^5\,3s4s$	
$2p^5 + 2p^5\,3s4p$	
$2p^5 + 2p^5\,3p4p$	
$2p^5 + 2p^5\,3p4d$	
$2p^5 + 2p^5\,3d4d$	
$2p^5 + 2p^5\,4s^2$	
$2p^5 + 2p^5\,4p^2$	
$2p^5 + 2p^5\,4d^2$	
$2p^5 + 2p^5\,4s4p$	
$2p^5 + 2p^5\,4p4d$	
$2p^5 + 2p^6\,3s$	Other ionic
$2p^5 + 2p^6\,3p$	
$2p^5 + 2p^6\,3d$	
$2p^5 + 2p^6\,4s$	
$2p^5 + 2p^6\,4p$	

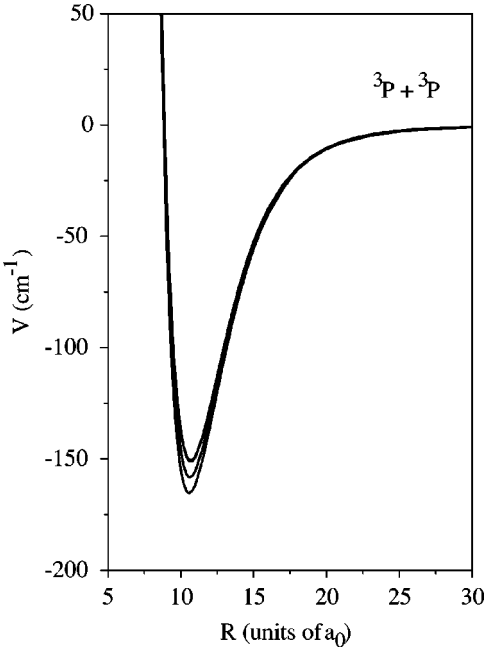

FIG. 1. $^5\Lambda_\sigma$ potential-energy surfaces of two interacting Ne atoms. The figure shows the potentials dissociating to the $2p^5\,3s + 2p^5\,3s$ atomic limits.

scribe the ''ionic'' properties at short internuclear separations.

The two classes labeled as ''other neutral'' and ''other ionic'' cannot contribute to the formation of the $S=2$ potential energy surfaces as for both classes there are only two active electrons, which can only form states with total electron spin zero or 1.

IV. $^5\Sigma$, $^5\Pi$, AND $^5\Delta$ STATES

In Fig. 1 and Table II we present the results of our calculations on the potentials belonging to the lowest $^5\Lambda_\sigma$ states of Ne_2. The six nearly degenerate quintet potentials correlate to the metastable $2p^5\,3s(^3P) + 2p^5\,3s(^3P)$ atomic limit. These are two $^5\Sigma_g$ and one $^5\Sigma_u$ state, one $^5\Pi_g$ and $^5\Pi_u$ state, and one $^5\Delta_g$ state. Several spectroscopic constants of these six curves are presented in Table II. All constants are found by fitting to the appropriate parts of the potentials. The quantity R_e is the internuclear separation at the deepest point of the curves, D_e is the dissociation energy or well depth at R_e relative to the potential energy at infinite internuclear separation, ω_e is the harmonic frequency at the deepest point, B_e is the rotational constant at R_e, and C_6 describes the long-range behavior of the potential. Effects due to other multipole terms could not be extracted from the long-range form of the *ab initio* potentials. In the table the curves are first ordered according to their symmetry and then their dissociation energy.

TABLE II. Spectroscopic constants of the $^5\Lambda$ potential curves dissociating to two metastable ^3P Ne atoms. R_e is in units of a_0, D_e, ω_e, and B_e are in cm^{-1} (1 cm^{-1} = 29.979 245 8 GHz), while C_6 is in units of $e^2a_0^5$ where $e = 1.60217733\times10^{-19}$ C is the electron charge.

State	g or u	D_e	R_e	ω_e	B_e	C_6 [a]
$^5\Sigma$	g	-165	10.6	25	0.054	3300
	g	-151	10.7	24	0.053	3100
	u	-150	10.7	24	0.053	3100
$^5\Pi$	g	-158	10.6	24	0.053	3200
	u	-158	10.6	24	0.053	3200
$^5\Delta$	g	-151	10.7	24	0.053	3000

[a]See note added in proof.

The long-range behavior of the metastable potential curves is dominated by an attractive induced dipole-dipole $-C_6/R^6$ potential. The six potentials have nearly identical C_6 coefficients since the two spherically symmetric $3s$ electrons of the metastable atoms dominate the long-range interactions. Small differences due to the orientation of the $2p^5$ orbitals relative to the internuclear axis, i.e., the projection Λ, are expected. In fact, from the last column of Table II we see that the C_6 coefficients are identical to within 10%. The value of the C_6 coefficients is predominantly determined by the mixing of the metastable molecule with the $2p^5\,3p + 2p^5\,3p$ configuration of the C_6 class of Table I. Our values of C_6 are about 50% larger than the values obtained in Ref. [3]. Their evaluation only considers the experimentally determined $2p^5\,3s$ to $2p^5\,3p$ transition dipole moments and therefore gives a lower bound to the value of C_6, whereas ours includes several ''C_6'' configurations.

A comparison between the Ne quintet potential and the ground-state $x^3\Sigma_u$ sodium dimer potential is illuminating. For both sodium and metastable Ne the outer $3s$ orbital dominates the electronic interactions and similarities in the shape of the potentials are expected. Moreover, for the quintet symmetry the electron spin of the electrons in the $2p^5$ orbital and the electron spin of the electron in the $3s$ orbital are aligned and hence we can compare the corresponding potentials with the spin-aligned $a^3\Sigma_u$ curve of Na_2. For the Na_2 $^3\Sigma_u$ curve the experimental equilibrium constants are $D_e = 173.8\,\text{cm}^{-1}$ and $R_e = 9.62a_0$ [21] and the dispersion coefficient is $C_6 = 1561e^2a_0^5$ [22]. Hence we see that the Ne quintet curves are slightly shallower at short internuclear separations, have a minimum at larger internuclear separation, and are more attractive at distances where the $-C_6/R^6$ dominates. The latter comes as no surprise as the atomic polarizability of metastable Ne is the larger of the two. The shallower wells are due to the additional correlation between the open $2p^5$ orbital and the $3s$ electrons.

The effect of the $\approx 10\,\text{cm}^{-1}$ splittings at R_e between the six quintet metastable curves on inelastic collisional rates is pronounced. For ultracold Na collisions the weak relativistic spin-spin dipole interaction lifts the electron-spin degeneracies of the $x^3\Sigma_u$ potential and ultimately limits the (collisional) lifetime of a gas of Na atoms due to depolarization [23]. These splittings for Na are $\sim 0.01\,\text{cm}^{-1}$ at R_e, which is orders of magnitude smaller than the nonrelativistic splittings calculated for neon. Hence we expect that depolarization rates of Ne($3s$) samples will be large.

In Fig. 2 we show the weights of the different classes of

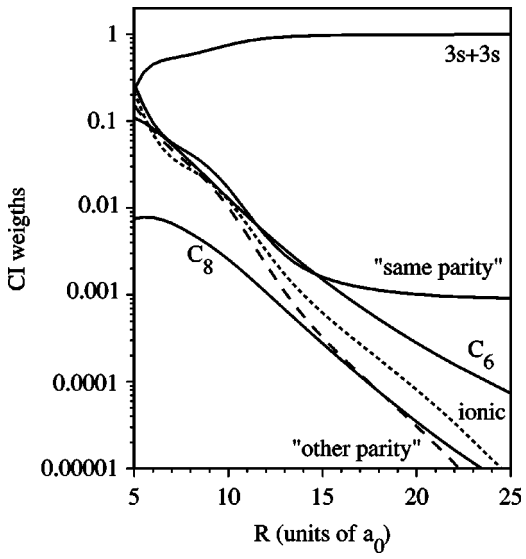

FIG. 2. The configuration weights of the $^5\Delta_g$ potential as a function of internuclear separation. The labels are defined in the text.

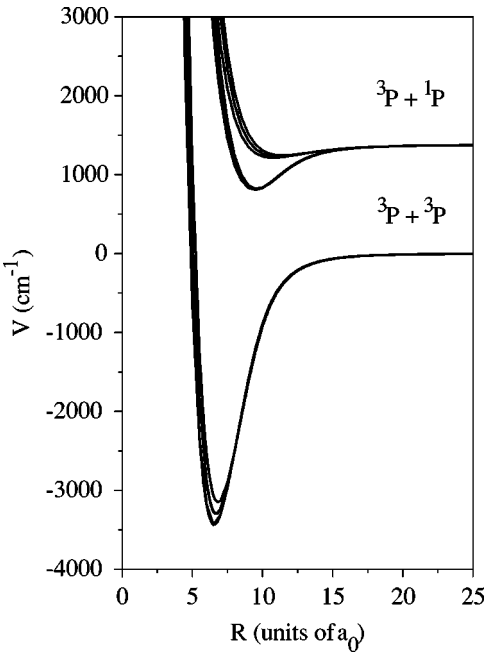

FIG. 3. $^3\Lambda_\sigma$ potential surfaces of two interacting metastable Ne atoms. The figure shows the potentials dissociating to the $2p^5\,3s + 2p^5\,3s$ atomic limits.

configurations, defined in Table I, of the $^5\Delta_g$ potential as a function of internuclear separation. The weights are defined as the sum of the squares of the CI coefficients of all the configurations contributing to a class. Hence, the figure illustrates the molecular formation. The dominant configuration for nearly all internuclear separations is the $2p^5\,3s + 2p^5\,3s$ configuration. This indicates that the atomic basis set in our generalized VB approach was a good starting point. At large internuclear separation the metastable configuration mixes with so-called ''same parity'' configurations. Together these configurations completely describe the dissociating atoms. The weights of the configuration belonging to the ''C_6'' and ''C_8'' class, which have a $1/R^6$ and $1/R^8$ dependency, respectively, are the first configurations that help form the molecule when the two atoms are brought together. This is consistent with the notion that at intermediate range internuclear separation the potentials are described by dispersion interactions. The weights of the ''opposite parity'' and ''ionic'' configurations have a nearly exponential behavior with internuclear separation, as both require an exchange of electrons between the two atoms. For $R<10a_0$ most classes contribute evenly to the molecular formation. Nevertheless nearly 50% of the weight of the CI expansion is due to the metastable configuration.

Quintet potential curves that dissociate to the ionic $Ne^+ + Ne^-$ limits lie above the metastable dissociation limit. This is consistent with the notion that the quintet symmetries do not autoionize. Remember that as discussed in Sec. III the classes ''other neutral'' and ''other ionic'' do not contribute to the formation of the metastable $S=2$ states.

V. $^3\Sigma$, $^3\Pi$, $^3\Delta$, AND $^1\Delta$ STATES

In Fig. 3 the 18 adiabatic triplet curves dissociating to the metastable $2p^5\,3s(^3P)+2p^5\,3s(^3P)$ and $2p^5\,3s(^1P) + 2p^5\,3s(^3P)$ limit are shown. Table III gives the most important spectroscopic constants for these curves. The curves are ordered by symmetry, followed by atomic dissociation limit and their dissociation energy with respect to this atomic limit. For example, the first group of curves with $^3\Lambda$ symmetry dissociates to the $^3P+^3P$ limit while the second group dissociates to the $^1P+^3P$ limit. The atomic asymptotic energy splitting between the nonrelativistic $E[2p^5\,3s(^1P)]$ and $E[2p^5\,3s(^3P)]$ state is approximately $1400\,\mathrm{cm}^{-1}$.

The eighteen $S=1$ curves separate into three bundles of lines. Within each group the variations are no more than a few percent. Notably the separation between the $^3\Pi_u$ and $^3\Pi_g$ within each group is small. In addition, the two $^3\Sigma_u$ curves for each of the three groups have several avoided crossings in the attractive regions of the potentials. For example, the two $^3\Sigma_u$ curves dissociating to the $^3P+^3P$ limit have an avoided crossing around $8a_0$. The two curves rapidly approach each other to within several cm^{-1} at a binding energy of $2500\,\mathrm{cm}^{-1}$. A Landau-Zener analysis [24] of this avoided crossing for two ultracold colliding atoms suggests that for a single pass through the region there is a near unity probability of jumping to the other curve.

The long-range C_6 coefficients of the triplet curves that dissociate to the $^3P+^3P$ limit are nearly equal to those of the $^5\Lambda$ curves. The C_6 values for the triplet curves that dissociate to the $^1P+^3P$ limit, however, are considerably larger. The dispersion potential is predominantly determined by mixing with the $2p^5\,3p+2p^5\,3p$ configuration and hence is determined by the atomic $2p^5\,3s(^{2S+1}P)$ to $2p^5\,3p(^{2S+1}L)$ transition moments [22]. Thus it follows for the nonrelativistic $2p^5\,3s$ Ne atom that the singlet-singlet transition dipole moments are larger than triplet-triplet dipole moments. As a consistency check the ratio between the con-

TABLE III. Spectroscopic constants of the $^3\Lambda$ and $^1\Delta_g$ potential curves dissociation to two metastable Ne atoms. For each symmetry the potentials are energy ordered and grouped according to their dissociation limits. R_e is in units of a_0, D_e, ω_e, and B_e are in cm^{-1}, while C_6 is in units of $e^2a_0^5$.

State	g or u	D_e	R_e	ω_e	B_e	C_6 [a]
$^3\Sigma$	g	-3437	6.6	132	0.140	3100
	u	-3432	6.6	132	0.140	3300
	u	-3151	6.8	129	0.129	3100
	g	-568	9.5	48	0.067	3900
	u	-567	9.5	49	0.068	4100
	u	-558	9.6	53	0.066	3900
	u	-163	10.7	24	0.052	3900
	g	-162	10.7	23	0.052	3900
	g	-133	11.4	21	0.046	4000
$^3\Pi$	g	-3300	6.7	131	0.135	3200
	u	-3291	6.7	131	0.134	3200
	u	-569	9.5	50	0.067	4100
	g	-567	9.5	50	0.067	4100
	g	-147	11.1	23	0.049	4000
	u	-146	11.1	23	0.049	4000
$^3\Delta$	u	-3434	6.6	132	0.140	3000
	u	-578	9.4	50	0.068	4200
	g	-162	10.7	24	0.052	4200
$^1\Delta$	g	-3523	6.6	131	0.139	3000
	g	-448	9.5	46	0.067	5300

[a]See note added in proof.

figuration weights of the $2p^5\,3p+2p^5\,3p$ configuration, which belongs to the ''C_6'' class, for a potential dissociating to the $^1P+^3P$ limit and a potential dissociating to the $^3P+^3P$ limit was evaluated for large internuclear separation and found to be consistent with the ratio between the corresponding C_6 coefficients.

Figure 4 shows the configuration weights of the lowest metastable $^3\Sigma_g$ curve as a function of internuclear separation. The CI weights for the ''ionic'' and ''other ionic'' have been combined into a single ''ionic'' line. The configuration weights of the various classes of this $^3\Sigma_g$ curve and the $^5\Delta_g$ potential in Fig. 2 have similar long-range trends. At short internuclear separation, differences exist. The most prominent difference is the increased contribution of the so-called ''ionic'' configurations inside $8a_0$. In fact, it reflects the presence of $[Ne^+(2p^5)+Ne^-]\,^3\Sigma_g$ potentials below the metastable limits of two metastable atoms, which are absent for the quintet symmetries. Physically this implies that the ionic complex $Ne^+(2p^5)+Ne(2p^6)$ plus a free electron can be formed or equivalently that the dimer autoionizes. Notice, that our ''ionic'' configurations are unable to predict the ionization width as in our basis this electron remains bound to the $Ne(2p^6)$ atom. Nevertheless, the ionic configurations do modify the shape of the potential curves.

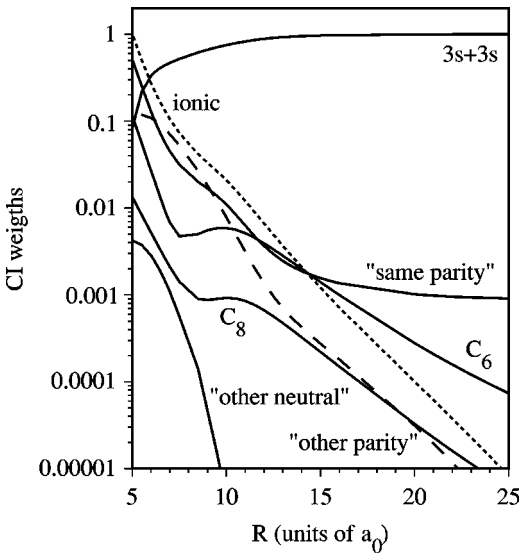

FIG. 4. The configuration weights of the lowest metastable $^3\Sigma_g$ potential as a function of internuclear separation. The labels are defined in the text.

A second difference between the CI weights presented in Figs. 2 and 4 is apparent at the bottom or deepest part of the potential. The $^3\Sigma_g$ curve has a smaller R_e than the $^5\Delta_g$ potential and we see for the $^3\Sigma_g$ potential that the metastable configuration contributes significantly less to the formation of the molecule at the bottom of the wells. Notice also that the configurations labeled ''other neutral'' contribute as well.

We conclude with describing representative singlet $S=0$ potentials. The adiabatic $^1\Delta$ curves dissociating to the meta-

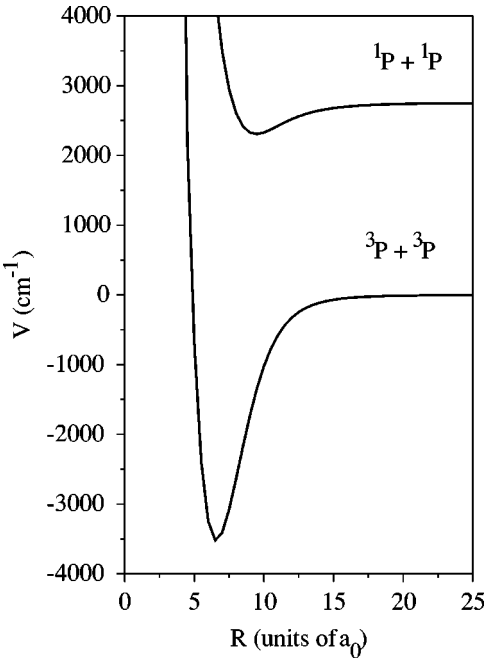

FIG. 5. $^1\Delta_\sigma$ potential surfaces of two interacting metastable Ne atoms. The figure shows the potentials dissociating to the $2p^5\,3s+2p^5\,3s$ atomic limits.

stable $2p^5\,3s(^3P)+2p^5\,3s(^3P)$ and $2p^5\,3s(^1P)+2p^5\,3s(^1P)$ limits are presented in Fig. 5. The two curves have g symmetry and the spectroscopic constants are presented in Table III. The long-range C_6 coefficient for the potential dissociating to the $^1P+^1P$ limit is significantly larger than the values for curves dissociating to the $^1P+^3P$ limit. Again this is due the larger dipole moment of the singlet-singlet transition.

VI. CONCLUSION

We have calculated *ab initio* nonrelativistic energy curves for two interacting metastable Ne atoms. From these curves we extracted dissociation energies, and other spectroscopic quantities as well as long-range dispersion coefficients. A comparison of $^5\Lambda$ potentials with the $a^3\Sigma_u$ sodium dimer potential showed a high degree of similarity in the shape of the potentials but also that differences are due to the larger correlation and polarization effects for a two-electron metastable neon atom. This is reflected in the multiplet structure of the $^5\Lambda$ potentials. For the $^3\Lambda$ and $^1\Delta$ potentials we find an even more complicated picture. There are two atomic limits and we find that the long-range C_6 coefficients for curves, dissociating to a limit where at least one of the atoms has a $2p^5\,3s(^1P)$ configuration, are much larger. Moreover, avoided crossings between curves of the same symmetry exist at short internuclear separation.

The molecular formation for a quintet and a triplet potential was studied while following configuration weights as a function of internuclear separation. Their radial behavior is understood by their long-range characteristics. At short range, ionic configurations were found to have a more important role for the triplet potential.

In order to obtain a more complete description of the metastable Ne_2, there is a need to implement spin-orbit interactions in the calculation. Additional improvements can be made by taking into account core-valence correlation effects, which are known to be very important in the alkali-metal dimers [25]. Unlike for the alkali-metal systems, experimental or theoretical guidance on the size of the correlation effects for metastable neon does not exist. We hope to address these issues in future publications.

Note added in proof. Recently, we further investigated the long-range properties of the metastable Ne dimer. Inclusion of all single-electron excitations out of the $2p^5$ shell leads to significantly smaller values of C_6. Other properties presented in the tables are not affected.

[1] C. Orzel, S. D. Bergeson, S. Kulin, and S. L. Rolston, Phys. Rev. Lett. **80**, 5093 (1998).

[2] M. R. Doery, E. J. D. Vredenbregt, S. S. Op de Beek, H. C. W. Beijerinck, and B. J. Verhaar, Phys. Rev. A **58**, 3673 (1998).

[3] M. R. Doery, E. J. D. Vredenbregt, J. G. C. Tempelaars, H. C. W. Beijerinck, and B. J. Verhaar, Phys. Rev. A **57**, 3603 (1998).

[4] G. V. Shlyapnikov, J. T. M. Walraven, U. M. Rahmanov, and M. W. Reynolds, Phys. Rev. Lett. **73**, 3247 (1994).

[5] D. Hennecart and F. Masnou-Seeuws, J. Phys. B **18**, 657 (1985).

[6] J. S. Cohen and B. Schneider, J. Phys. B **61**, 3230 (1974).

[7] W. Heitler and F. London, Z. Phys. **44**, 455 (1927).

[8] R. McWeeny, *Methods of Molecular Quantum Mechanics*, 2nd ed. (Academic Press, London, 1978).

[9] C. C. J. Roothaan, Rev. Mod. Phys. **23**, 69 (1951); **32**, 179 (1960).

[10] S. Huzinaga, Phys. Rev. **122**, 121 (1961).

[11] E. Clementi and A. Veillard, J. Chem. Phys. **44**, 3050 (1966).

[12] W. A. Goddard III, Phys. Rev. **157**, 81 (1967).

[13] W. A. Goddard III; and R. C. Ladner, J. Am. Chem. Soc. **93**, 6750 (1971).

[14] W. J. Hunt, P. J. Hay, and W. A. Goddard III, J. Chem. Phys. **57**, 738 (1972).

[15] P. J. Hay, W. J. Hunt, and W. A. Goddard III, Chem. Phys. Lett. **13**, 30 (1972); S. L. Guberman and W. A. Goddard III, Phys. Rev. A **12**, 1203 (1975); B. J. Moss and W. A. Goddard III, J. Chem. Phys. **63**, 3523 (1975); L. B. Harding and W. A. Goddard III, J. Am. Chem. Soc. **97**, 6293 (1975).

[16] S. Kotochigova and I. Tupitsyn, Int. J. Quantum Chem. **29**, 307 (1995).

[17] S. Kotochigova and I. Tupitsyn, J. Res. Natl. Inst. Stand. Technol. **103**, 201 (1998).

[18] S. Kotochigova and I. Tupitsyn, J. Res. Natl. Inst. Stand. Technol. **103**, 205 (1998).

[19] A. I. Sherstyuk, Opt. Spectrosc. **38**, 601 (1975).

[20] A. I. Sherstyuk and P. F. Gruzdev, Opt. Spectrosc. **42**, 690 (1977).

[21] W. T. Zemke and W. C. Stwalley, J. Chem. Phys. **100**, 2661 (1994).

[22] P. Kharchenko, J. F. Babb, and A. Dalgarno, Phys. Rev. A **55**, 3566 (1997).

[23] E. Tiesinga, S. J. M. Kuppens, B. J. Verhaar, and H. T. C. Stoof, Phys. Rev. A **43**, 5188 (1991).

[24] N. F. Mott and H.S.W. Massey, *Atomic Collisions* (Oxford University Press, New York, 1965); E. E. Nikitin, *Theory of Elementary Atomic and Molecular Processes in Gases* (Clarendon Press, Oxford, 1974).

[25] M. Krauss and W. J. Stevens, J. Chem. Phys. **93**, 4236 (1990).